Extracellular Bacterial Synthesis of Protein-Functionalized Ferromagnetic Co_3O_4 Nanocrystals and Imaging of Self-Organization of Bacterial Cells under Stress after Exposure to Metal Ions

Umesh Kumar,[†,△] Ashvini Shete,[†] Arti S. Harle,[‡] Oksana Kasyutich,[§] W. Schwarzacher,[§] Archana Pundle,*[,†] and Pankaj Poddar*[,△]

Biochemical Science Division, National Chemical Laboratory, Pune 411008, India; Center for Materials Characterization, National Chemical Laboratory, Pune 411008, India; H.H. Wills Physics Laboratory, University of Bristol, Tyndall Avenue, Bristol BS8 1TH, U.K.; and Materials Chemistry Division, National Chemical Laboratory, Pune 411 008, India

Received September 24, 2007. Revised Manuscript Received November 22, 2007

Co_3O_4, which crystallizes in the spinel phase at temperatures much higher than ambient temperatures, orders antiferromagnetically below its Neel temperature (~40 K). However, in nanosize, it shows ferromagnetic ordering due to surface canting, disorder, imperfect oxygen atom coordination, etc. Here, for the first time, we report the synthesis of single-crystalline, ferromagnetic Co_3O_4 nanoparticles functionalized with proteins (size 5–7 nm) using cobalt acetate as precursor at room temperature in aqueous medium by a metal-tolerant marine bacterium isolated from the coast of the Arabian Sea. Energetically unfavorable change in the oxidation state of Co atoms from (+2 to +3) during synthesis by the bacterial strain was evidenced by X-ray photoelectron spectroscopy. The effect on the morphology of bacterial cells after exposure to the cobalt acetate was imaged by scanning electron microscopy showing cooperative, self-organized, structured colony formation, possibly due to the interbacterial communication under external stress.

1. Introduction

The microbial activity is known to be responsible for the transformation of at least one-third of the elements in the periodic table.[1] These transformations are the result of assimilatory, dissimilatory, or detoxification processes and form the cornerstones of many biogeochemical cycles involving the change in the valence states (i.e., oxidation/reduction) or chemical form (i.e., solid, liquid, gas) of elements.[1] Metals play an integral role in the life processes of microorganisms. Some metals, such as calcium, cobalt, iron, potassium, sodium, etc., are required as nutrients and are essential since they function as the catalysts for biochemical reactions, stabilizers of protein structures and bacterial cell walls, serve in maintaining osmotic balance, involve in redox processes, or stabilize various enzymes and DNA through electrostatic forces.[2] Marine water and sediments contain a lot of metal salts which are naturally present or enter into the marine environment as a contaminant through dumping of huge amount of industrial and domestic waste containing salts of lead, arsenic, cadmium, nickel, cobalt, mercury, silver, etc.[3] Therefore, high metal tolerance, among marine bacteria, is a common phenomenon which makes them ideal model candidates for exploring metal/metal oxide nanoparticle synthesis in the laboratory environment.[4]

Very recently, the microbial synthesis of inorganic materials including noble metals, alloys, binary oxides, and ternary oxides using fungi, yeast, bacteria, and a variety of other microorganisms has gained popularity.[5–7] The reason being in their obvious advantages over the traditional wet-chemical methods, where at several times the synthesis methodology requires expensive organometallic precursors, high temperature and pressure, and hazardous chemicals and solvents. On the other hand, the reduction of metal ions in nature by microbes is done in ambient conditions. In this "green synthesis route", the as-synthesized particle surface is inherently functionalized by the proteins which give them specific advantages. Because of this inherent and robust biofuctionalization, the as-synthesized particles form stable suspension in the aqueous medium, and further coating of biomolecules becomes easier. The protein layer also prevents particles surfaces fusing together directly, although the

* Corresponding authors. E-mail: av.pundle@ncl.res.in, p.poddar@ncl.res.in.
† Biochemical Science Division, National Chemical Laboratory.
‡ Center for Materials Characterization, National Chemical Laboratory.
§ University of Bristol.
△ Materials Chemistry Division, National Chemical Laboratory.

(1) Stolz, J. F.; Basu, P.; Oremland, R. S. *Int. J. Microbiol.* **2002**, *5*, 201.
(2) Bruins, M. R.; Kapil, S.; Oehm, F. W. *Ecotoxicol. Environ. Saf.* **2000**, *45*, 198.
(3) *Our Planet, Our Health*, Report of the World Health Organization on Health and Environment; Oxford University Press: Oxford, 1992.
(4) Sabry, S. A.; Ghozlan, H. A.; Abou-Zeid, D. M. *J. Appl. Microbiol.* **1997**, *82*, 245.
(5) Bharde, A.; Wani, A.; Shouche, Y.; Pattayil, A. J.; Prasad, B. L. V.; Sastry, M. *J. Am. Chem. Soc.* **2005**, *127*, 9326.
(6) Bansal, V.; Poddar, P.; Ahmad, A.; Sastry, M. *J. Am. Chem. Soc.* **2006**, *128*, 11958.
(7) Kowshik, M.; Ashtaputre, S.; Kharrazi, S.; Vogel, W.; Urban, J.; Kulkarni, S. K.; Paknikar, K. M. *Nanotechnology* **2003**, *14*, 95.

10.1021/cm702727x CCC: $40.75
Published on Web 01/31/2008

particles tend to agglomerate due to the protein–protein interactions. In fact, in contrast to the surfactant-passivated magnetic nanoparticles synthesized by traditional methods, the protein-functionalized particles are more likely to behave as isolated particles due to relatively thicker coating of proteins which prevents interparticle interactions. These particles can be easily dried out of aqueous medium to form powder and can be resuspended without agglomeration.

However, similar to any other synthesis route, the microbial synthesis comes with several challenges which are yet to be explored and solved such as better control over size and shape, scaling up of the synthesis to get large amount of nanomaterials, and synthesis of complex oxide materials with desired phases. Chemical synthesis of nanomaterials, on the other hand, has already advanced to provide excellent control over size and shape. Another challenge, in the case of the microbial technique, is to fully understand the synthesis mechanism at the molecular level, which eventually may help in providing better control over size and shapes as well as crystallinity in the future.

In this article, learning from nature's own sustainable way of remediation of the metal ions, we have utilized a marine bacterium culture (obtained from the Arabian sea coast) in the laboratory environment to synthesize spinel structured, crystalline Co_3O_4 nanoparticles, as a model system, after exposing bacteria to the aqueous solution of cobalt acetate in ambient conditions. Out of 15 bacterial strains isolated from the marine water and sediment sample, only three bacterial strains showed resistance to cobalt after exposing them to Co acetate (used as a precursor in this study for the synthesis of Co_3O_4 nanoparticles). Furthermore, only one strain gave us the visible indication of the formation of nanoparticles (appearance of turbidity), and other two strains did not give us any positive result. Details about the isolation of bacterial strain and synthesis of Co_3O_4 particles are provided in the Supporting Information. The Co_3O_4 particles formed by this method are inherently passivated by the bacterial proteins. Co_3O_4 is known to have a normal cubic spinel structure and is antiferromagnetic in the bulk form with the Neel temperature T_N between 30 and 40 K.[8] However, in the nanoregime, uncompensated spins at the particle surfaces can become a large fraction of the total number of spins, thereby giving overall ferromagnetic-type behavior. Magnetic nanoparticles have aroused enormous interest owing to their unique size- and shape-dependent properties and potential applications, e.g., magnetocaloric refrigeration, read-head sensors, magnetic storage media, as filler materials in polymers in electromagnetic shielding applications, magnetorheological devices, etc.[9–13] There are various wet-chemical methods reported to synthesize the

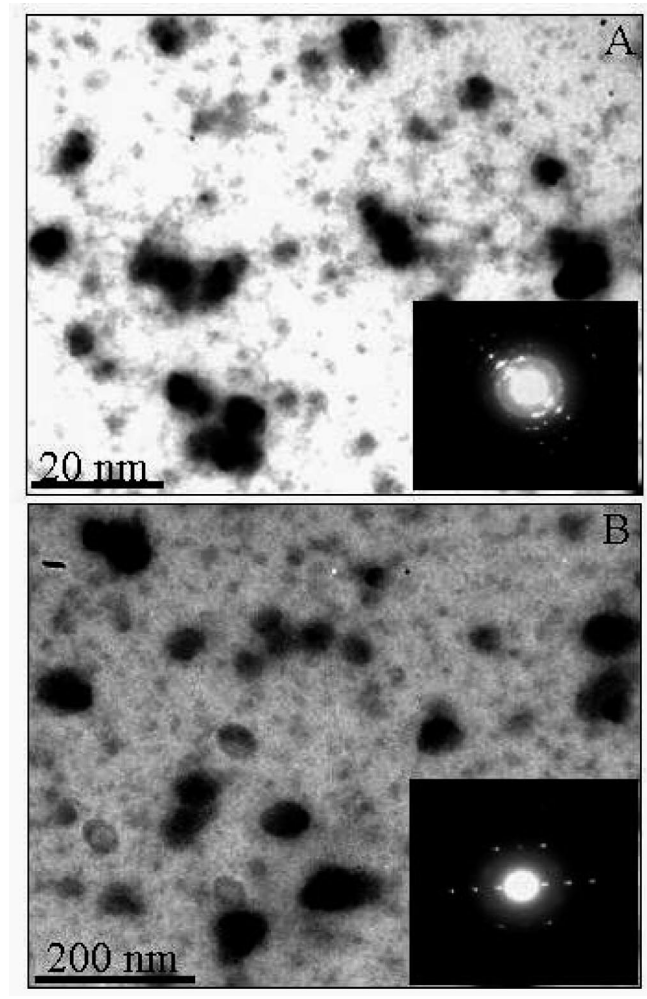

Figure 1. TEM micrographs of as-synthesized (panel A) and calcined (panel B) Co_3O_4 nanoparticles. In the inset, we have shown selected area diffraction (SAED) patterns.

Co_3O_4 nanoparticles; however, to the best of our knowledge, there is no report on the microbial synthesis of Co_3O_4. We believe that any previous attempts for the microbial synthesis of this material (or even Co nanoparticles) could have failed due to the toxicity of the Co ions toward previously used bacterial, fungi cultures. Moreover, it should be noted that when it comes to the microbial synthesis of the magnetic nanoparticles, γ-Fe_2O_3 and Fe_3O_4 are the only materials which are previously reported in the literature.[5]

2. Results and Discussion

To analyze the size and shape of the particles at a broader range, we have shown TEM images (presented in Figure 1) on both as-synthesized (panel A) and calcined nanoparticles (panel B). The top panel shows that the as-synthesized particles seem to be agglomerate (due to protein-functionalized surfaces) with average size of the quasi-spherical particles around 6 nm. The robust protein coating, on one hand, helps the agglomeration due to the interprotein linkage and, on the other hand, prevents the Co_3O_4 particles surfaces to fuse together to have exchange interaction, thereby keeping their identity as an isolated nanoparticle intact. After mild calcination (200 °C for 2 h), it appears that the particles get further agglomerated, and the size of these agglomerates

(8) Roth, W. L. *J. Phys. Chem. Solids* **1964**, *25*, 1.
(9) Poddar, P.; Sahoo, Y.; Srikanth, H.; Prasad, P. N. *Appl. Phys. Lett.* **2005**, *87*, 062506.
(10) Poddar, P.; Fried, T.; Markovich, G.; Sharoni, A.; Katz, D.; Wizansky, T.; Milo, O. *Eur. Phys. Lett.* **2003**, *64*, 98.
(11) Poddar, P.; Fried, T.; Markovich, G. *Phys. Rev. B* **2002**, *65*, 172405.
(12) Poddar, P.; Wilson, J. L.; Srikanth, H.; Yoo, Y. H.; Wereley, N. M.; Kotha, S.; Barghouty, L.; Radhakrishnan, R. *J. Nanosci. Nanotechnol.* **2004**, *4*, 192.
(13) Poddar, P.; Wilson, J. L.; Srikanth, H.; Morrison, S. A.; Carpenter, E. E. *Nanotechnology* **2004**, *15*, S570.

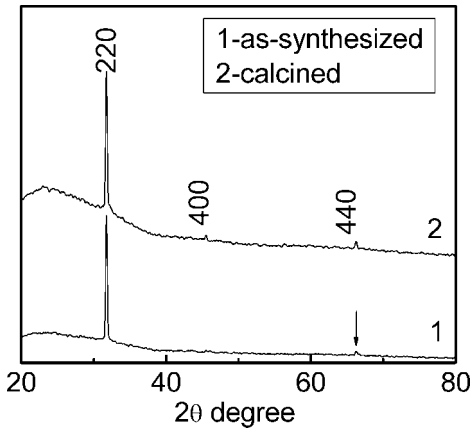

Figure 2. Powder XRD pattern of as-synthesized (curve 1) and calcined (curve 2) Co_3O_4 nanoparticles.

increases to around 50 nm as at this temperature proteins start degrading and clumping together. We believe that inside the agglomerated mass the Co_3O_4 nanoparticle surfaces still remain isolated due to the coating and actual particle sizes are much smaller. The selected area electron diffraction (SAED) patterns (presented in the insets of both the panels) show a dot pattern indicating very good single crystallinity, consistent with the XRD patterns.

As we mentioned earlier, Co_3O_4 has a normal spinel structure which shows antiferromagnetic ordering below 40 K. Co_3O_4 unit cells contain 8 Co^{2+} at tetrahedral A sites and 16 Co^{3+} at octahedral B sites with zero moment because of the large crystal field splitting of the 3d orbitals by the octahedral cubic field. The Co^{2+} ions at the tetrahedral sites show magnetic moments of 3.25 μ_B per ion.[14] In Figure 2, we have shown the powder XRD pattern for as-synthesized as well as calcined (at 200 °C for 2 h) samples. It is interesting to note that the XRD pattern for the as-synthesized sample (curve 1) shows only two well-defined peaks corresponding to ⟨220⟩ and ⟨440⟩ planes. The peak corresponding to ⟨220⟩ is most intense in our case. However, for a nontextured, polycrystalline sample, the ⟨331⟩ peak situated at ⟨121⟩ = 36.7° shows the highest intensity, and the peak situated at ⟨220⟩ is the second highest intense peak (PCPDF# 78-1970, 43-1003). The absence of ⟨331⟩ as well other (relatively less intense) peaks indicates highly oriented growth of the nanocrystals toward ⟨220⟩ plane. After calcination (curve 2), we find that the peak at ⟨440⟩ becomes more pronounced, and another peak corresponding to the ⟨400⟩ plane emerges. The lattice constant (8.0 Å) calculated from our XRD data matches with the value reported in literature for bulk Co_3O_4.[8] To further confirm the crystallinity and shape of the particles, we used high-resolution transmission electron microscopy (HR-TEM). In Figure 3, we have shown the HR image (panel A) and SAED pattern (panel B) of the as-synthesized particle. In panel A, we could see clearly highly crystalline lattice even for as-synthesized particles with lattice-plane corresponding to ⟨311⟩ with *d* value of 2.4 Å (highest intense) which was not seen in the XRD pattern (Figure 2). The SAED image (panel B) shows a nice dot pattern indexed for ⟨400⟩ and ⟨440⟩ planes. In Figure 3C−E, we have shown HR-TEM images and SAED pattern for the calcined particles. Here, panels C and D again show highly crystalline particles with lattice planes ⟨311⟩ and ⟨220⟩ (corresponding to the most intense and second most intense peaks reported for bulk Co_3O_4). The SAED pattern (panel E) could be indexed for ⟨331⟩ and ⟨440⟩. Here it is quite interesting to note that phase formed by the microbial method is quite pure as we do not get any indication of CoO phase. We believe that this is probably due to the fact that at room temperature the formation of Co_3O_4 is thermodynamically favorable,[15] and only after heating Co_3O_4 above 930 °C (in reducing environment), it gets transformed into CoO phase.[15]

To further investigate the formation of Co_3O_4 phase as well as presence of proteins, we used X-ray photoemission spectroscopy, which is a highly surface sensitive technique. As-obtained XPS core level spectra were background-corrected using the Shirley algorithm, and chemically distinct species were resolved using a nonlinear least-squares fitting procedure. The core level binding energies (BE) were aligned with the carbon binding energy of 285 eV. In Figure 4, we have compared the background-corrected XPS spectra for as-synthesized (panels A−D) and calcined (panels E−H) Co_3O_4 nanoparticles. In (Figure 4A), the carbon 1s core level spectra shows well-defined (deconvoluted) peaks at the binding energies 282, 285, 286, and 288 eV, where the peak at 285 eV is due to the C 1s core level transition originating from hydrocarbon chains and subsequent peaks situated at 286 and 288 eV are due to the presence of α-carbon and −COOH groups present in the proteins, respectively.[16] The peak at lower binding energy of ∼282 eV indicates the presence of aromatic carbon due to the protein. It should be noted that after calcination (panel E) the peak at 286 eV disappears due to the partial removal/degradation of the proteins. Panels B and F show N 1s core level spectra for as-synthesized and calcined samples where the peak at 398 eV is due to the N 1s core level transitions and the peak at 400 eV is due to possible cationic state of nitrogen present in protein−nanoparticle complex. The peaks at 532 eV shown in panels C and G correspond to the O 1s core level transition. The peaks shown in panels D and H correspond to Co 2p core level spectra indicating the presence of four peaks at BE around 782, 788, 797, and 803 eV. Among these peaks, the peaks at BE 782 and 797 eV are due to spin–orbit splitting in the 2p level—$2p^{3/2}$ and $2p^{1/2}$ correspondingly with an energy gap of 15 eV. It should be noted here that shift of the peaks $2p^{3/2}$ and $2p^{1/2}$ from 778 and 793 eV correspondingly to the higher binding energies indicates absence of Co metal.[17] The remaining peaks at 789 and 804 eV are satellite peaks which are weaker in intensity.[18,19] For the octahedrally coordinated cobaltous ion (Co^{2+}), the $2p^{3/2}$ peak is split by

(14) Ichiyanagi, Y.; Yamada, S. *Polyhedron* **2005**, *24*, 2813.
(15) Wu, R. J.; Wu, J. G.; Tsai, T. K.; Yeh, C. T. *Sens. Actuators, B* **2006**, *120*, 104.
(16) Bansal, V.; Rautaray, D.; Bharde, A.; Ahire, K.; Sanyal, A.; Ahmad, A.; Sastry, M. *J. Mater. Chem.* **2005**, *15*, 2583.
(17) Girardon, J.; Lermontov, A. S.; Gengembre, L.; Chernavskii, P. A.; Griboval-Constant, A.; Khodakov, A. Y. *J. Catal.* **2005**, *230*, 339.
(18) Oku, M.; Hirokawa, K. *J. Electron Spectrosc. Relat. Phenom.* **1976**, *8*, 475.
(19) Hirokawa, K.; Honda, F.; Oku, M. *J. Electron Spectrosc. Relat. Phenom.* **1975**, *6*, 333.

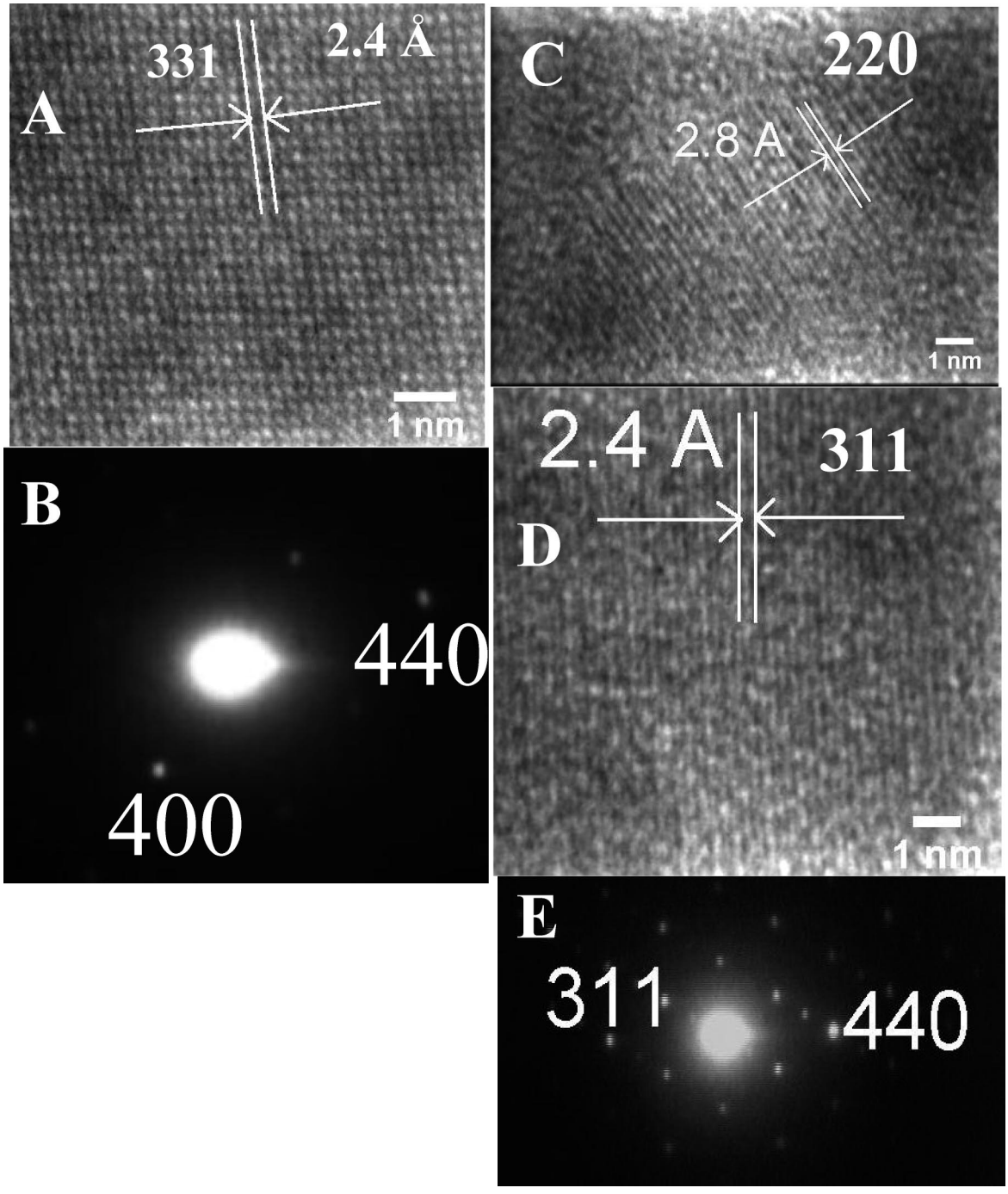

Figure 3. HR-TEM images and selected area diffraction (SAED) patterns for as-synthesized Co_3O_4 nanoparticles (panels A, B) and for calcined nanoparticles (panels C, D, E).

nearly 6.2 eV to form a satellite peak at 788.2 eV and for the tetrahedrally coordinated one; the splitting is around 5.3 eV to form the satellite peak at 787.3 eV.[18,19] In our case, these two satellite peaks are seen as a broad peak situated at around 788 eV. On the other hand, for Co $2p_{1/2}$ levels, both 6- and 4-fold coordination ions have about 6.2 eV satellite splitting which gives the satellite peak at around 803.2 eV as seen in our case also. Overall, the Co 2p spectrum for Co_3O_4 is considered to be the sum of spectra of Co^{2+} and Co^{3+} ions. A comparison between the panels D and H show that after calcination (panel H) the peaks become more intense. To further investigate the presence of Co^{3+} ions in microbial synthesized Co_3O_4, we decided to compare D and H with the XPS spectra of Co acetate shown in panel I. In sharp contrast, we can see that the peaks in the precursor molecule (due to just Co^{2+}) are quite sharp in comparison to D and H where the peaks are quite broad, which indicates that the peak broadening in D and H is due to the contribution from Co^{3+} as well as due to the change in the chemical environment.

Here it worth mentioning that, in contrast to other neighboring spinels such as Fe_3O_4 and Mn_3O_4, Co_3O_4 is thermodynamically stable at room temperature (surfaces of Fe_3O_4 and Mn_3O_4 readily convert to Fe_2O_3 and Mn_2O_3, respectively). In the case of Fe_3O_4 and Mn_3O_4, XPS may not show a contribution from Fe^{3+} and Mn^{3+}; however, on

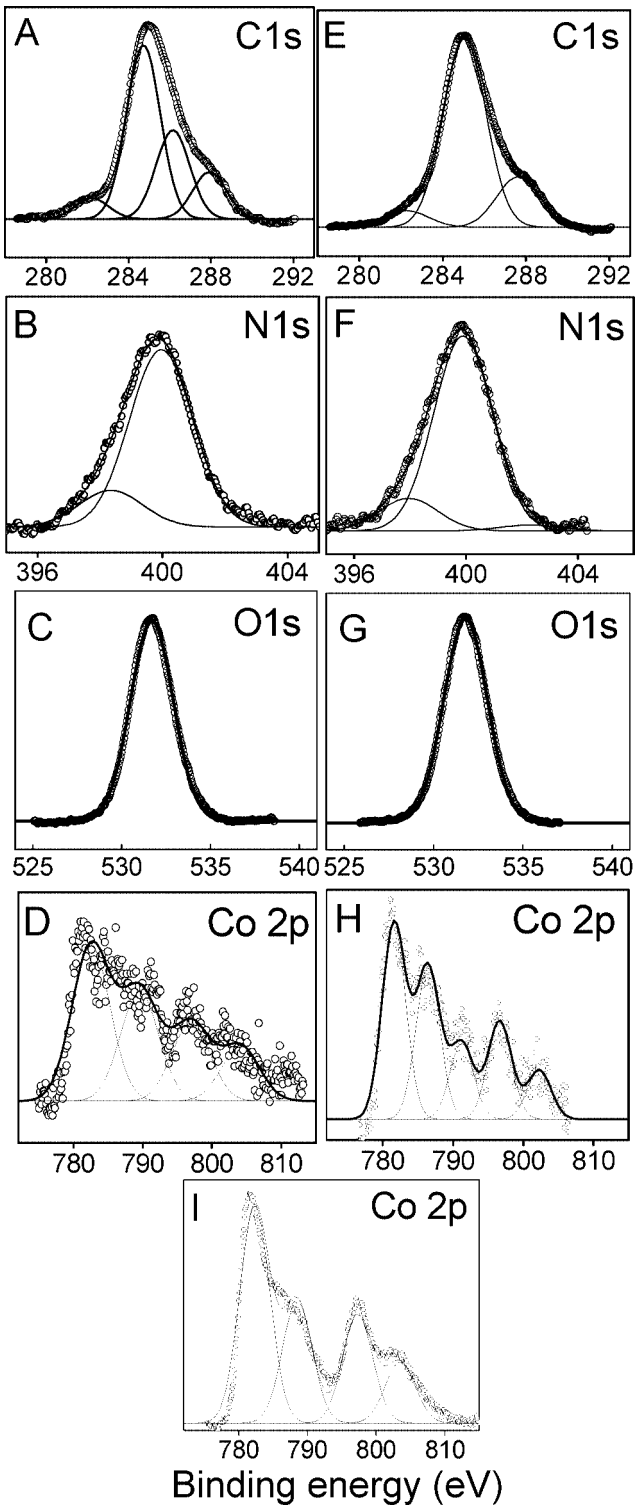

Figure 4. XPS spectra of as-synthesized (A−D), calcined (E−H) Co_3O_4 nanoparticles, and Co acetate (I). The solid lines show deconvoluted curve-fits.

the other hand, Co_3O_4, being a stable phase, does show a peak corresponding to Co^{3+} as discussed above.[18,19] Another reason behind the contribution of Co^{3+} is that Co^{2+} are located at the tetrahedral sites (A) giving net magnetic moment, and Co^{3+} ions (diamagnetic) occupy octahedral B-sites; therefore, due to the absence of any interaction between both of these ions in photoelectron emission process, they should give intrinsically different spectral lines which are seen as a broadened peak in our case.[18,19]

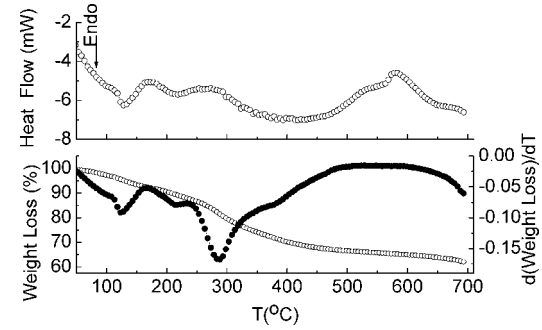

Figure 5. TGA and DTA curves of biologically synthesized Co_3O_4 nanoparticles.

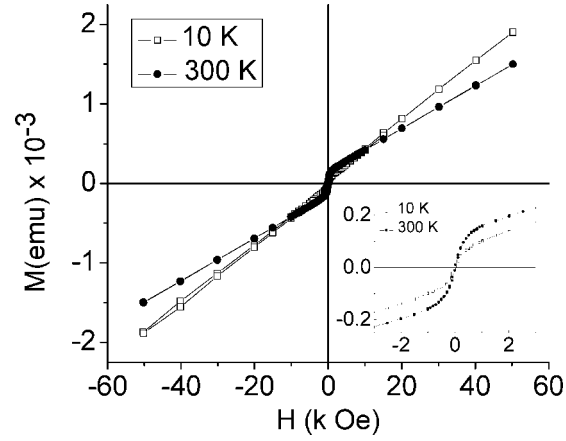

Figure 6. Graph showing magnetization vs magnetic field measurements of biologically synthesized Co_3O_4 (calcined) nanocrystals at 10 and 300 K. The inset shows a zoom view.

We used thermogravimetric analysis (TGA) and differential thermal analysis (DTA) on as-synthesized Co_3O_4 nanoparticles from room temperature to 700 °C to investigate the presence of protein at the nanoparticle surfaces, unreacted Co acetate, and structural stability of Co_3O_4 phase at higher temperatures. The results are shown in Figure 5. As we have mentioned earlier, Co_3O_4 nanoparticle surfaces are inherently functionalized with a robust layer of biomolecules as supported by TGA curve that indicates nearly 30% weight loss during heating the particles from room temperature to 400 °C (attributed to the loss of moisture and degradation of proteins) associated primarily with the endothermic heat flow. The DTA data rules out the presence of unreduced Co acetate in our samples. It should be noted that Co acetate shows a strong characteristic exothermic peak at around 225 °C due to the combustion of acetate which is absent in our data (Figure 5),[19] concluding the absence of any unreacted precursor. We believe that overall endothermic behavior as seen in Figure 5 is due to the decomposition of proteins.

Now it is interesting to check the magnetic properties of the Co_3O_4 nanoparticles. As discussed above, Co_3O_4 is known to have a normal cubic spinel structure and is antiferromagnetic in the bulk form with the Neel temperature T_N between 30 and 40 K.[8] However, in the nanosize, uncompensated spins at the particle surfaces can become a large fraction of the total number of spins thereby giving overall ferromagnetic-type behavior, confirming that we performed magnetization vs magnetic field loop measurements at 10 and 300 K for as-synthesized and calcined

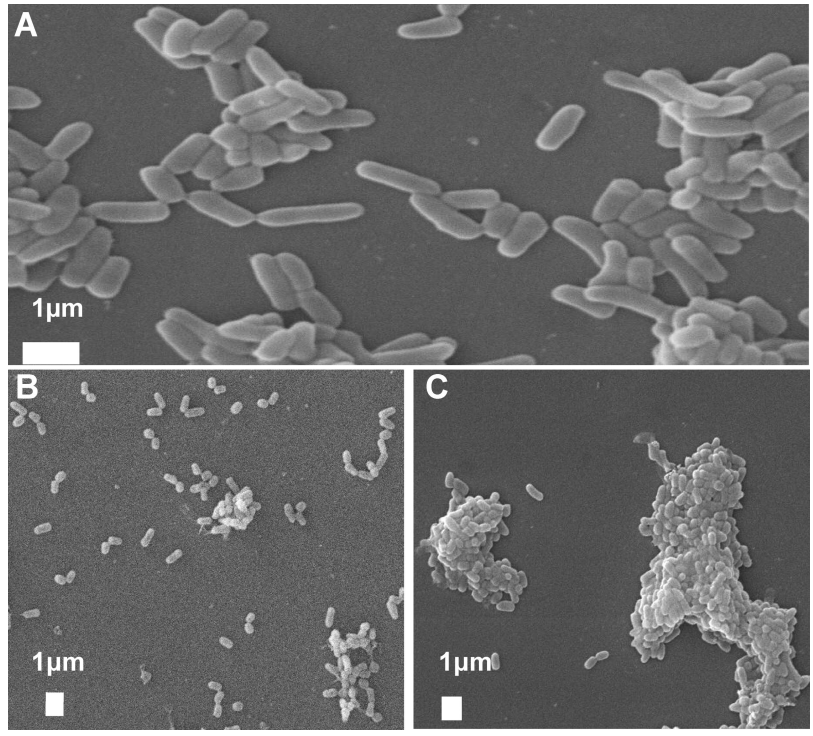

Figure 7. SEM images showing morphology of "control" bacterial sample initially (panel A) and after 24 h (panel B). Panel C shows bacterial sample 24 h exposing them to Co acetate.

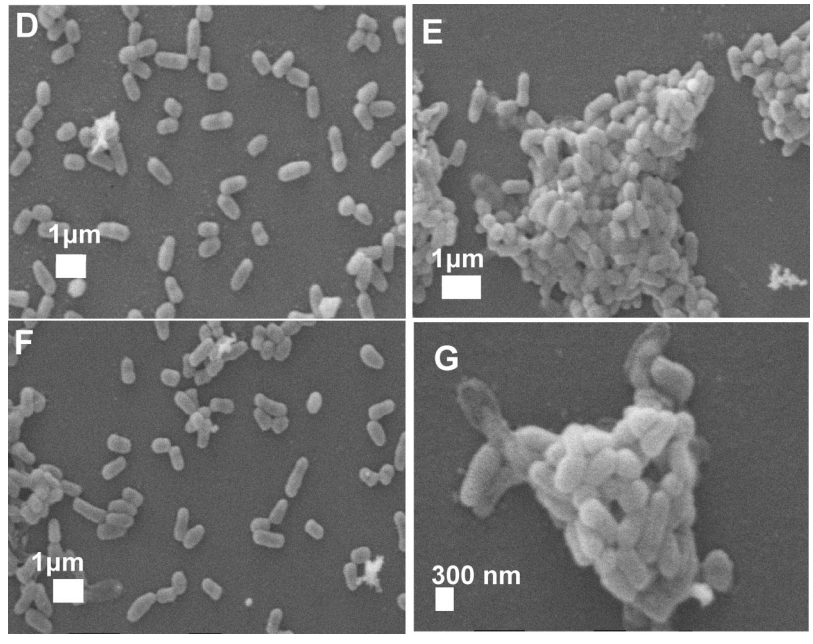

Figure 8. SEM images showing morphology of "control" bacterial sample after 48 h (panel D) and after 72 h (panel F). Panels E and G show bacterial samples taken 48 and 72 h after exposing them to Co acetate, respectively.

samples. However, the as-synthesized sample shows dominantly diamagnetic background due to the protein and water content. The $M-H$ loop on calcined sample (Figure 6) shows nonlinear reversible behavior at 10 and 300 K with increase in the moment at 10 K. The $M-H$ curves do not show any saturation until the highest applied field of 50 kOe which is due to the surface spin disorder, canting, etc. The reason of nonzero net moment and ferromagnetic-type behavior in nanosize is mainly due to the nonzero moments of Co^{3+} ions at octahedral sites which is in turn due to the lattice defects (missing oxygen atoms) as well as the distortion of the crystal symmetry. Other reasons for nonzero magnetic moment in antiferromagnetic nanoparticles can be attributed to uncompensated spins, spin disorder, and canted spins at the surface of the particles.[20]

Now the question arises, what is the mechanism by which the synthesis of Co_3O_4 (instead of CoO or Co nanoparticles) might be taking place? It is remarkable to note that here we used Co acetate as precursor where the Co is in the +2

(20) Jacob, E. B.; Cohen, I.; Golding, I.; Gutnick, D. L.; Tcherpakov, M.; Helbing, D.; Ron, I. G. *Physica A* **2000**, *282*, 247.

oxidation state. But, to form a unit cell of Co_3O_4, among total 24 Coions, only 8 ions are in Co^{2+} and rest of the 16 ions are in Co^{3+} form which means that the bacterium is involved somehow in changing the oxidation state of Co from +2 to +3, which is quite surprising. To understand the mechanism, it is required to answer the following questions: (1) What compels the bacterium to change the oxidation state of Co ions from +2 to +3? (2) Is it required for their survival? (Is the Co^{3+} state is less toxic to them?) (3) Which biomolecules are responsible for this reaction? The reduction potential of Co^{3+} to Co^{2+} state is 1.81 eV; therefore energetically, it is favorable to oxidize Co^{3+} to Co^{2+} (not the other way round). However, it is surprising that in our case the bacterium is capable of oxidizing Co^{2+} ions to Co^{3+} state. This also supports our hypothesis that Co^{3+} ions are formed by bacteria only, and they are not formed spontaneously in the reaction mixture. It also worth noting that the reduction potential of Co^{2+} to Co^0 is −0.28 eV, which does not allow reduction to take place spontaneously.

To fully understand the biochemical origin of synthesis mechanism, it is important to identify the strain up to the species level responsible for the oxidation. For this purpose, we used the 16S rRNA oligonucleotide cataloguing technique. Phylogenetic analysis of the 16S rRNA gene sequence of strain AP6 revealed an affiliation of the strain with *Brevibacterium casei* (Supporting Information). According to the current understanding, in most of these biosynthesis processes, precursor salts are either hydrolyzed or reduced, and the proteins responsible for these processes are generally cationic in nature.[16] Heavy metals are disseminated through the environment as part of a natural planetary biogeochemical activity and have been adopted by the biological systems because of their catalytic versatility, but their reactivity turns them toxic even at very low concentrations. Their toxicity in connection with their nonspecific intake by different channels and transporters has forced the organisms living in contact with these metals to develop systems to tightly control metal-ion homeostasis and resistance.[21] Heavy metal resistance in bacteria is the result of multiple resistance systems, and different mechanisms are displayed by different organisms, probably depending on the niche from which the organism has been isolated. Different mechanisms are responsible for conferring cobalt resistance. The first mechanism includes the members of the resistance-nodulation-cell division (RND) protein family which helps in export of superfluous cations. This system is known as the CzcCBA efflux system which is responsible for efflux of Co^{2+}, Zn^{2+}, Cd^{2+}, and Ni^{2+}. Similar to CzcCBA, two different homologous systems have been reported, i.e., Cnr operon and *rcnA* locus which confers resistance to cobalt and nickel[22,23] and ncc locus which confers resistance to cobalt, nickel, and cadmium.[24] The second mechanism is cation diffusion facilitator (CDF family) which serves as secondary cation filters in bacteria. Primary substrates of CDF proteins are Zn^{2+}, Co^{2+}, Ni^{2+}, Cd^{2+}, and Fe^{2+}.[25] In all these mechanisms, it has been proposed that Co^{2+} is the ion moiety which goes inside the cell and comes out through efflux pump. Here we report for the first time that Co^{2+} was supplied to the biological system in the form of cobalt acetate, but the nanoparticles formed showed the presence of both Co^{2+} and Co^{3+}ions as discussed above. We believe that the change in the oxidation state is either due to one of the mechanisms discussed above or because of a totally new hitherto unknown mechanism working in *Brevibacterium casei*. Such type of oxidation mechanism has been reported for other metals as well; for example, arsenite oxidase converts As(III) to As(V) and arsenate reductase converts As(V) to As(III).[26]

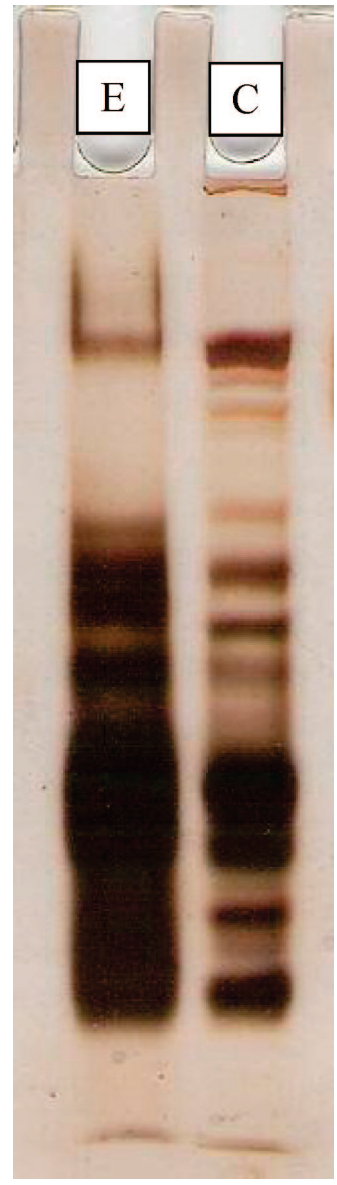

Figure 9. Protein profile comparison from the supernatant collected from the culture flask of Brevibacterium with salt (E) and without salt (C).

(21) Checa, S. K.; Espariz, M.; Audero, M. E.; Botta, P. E.; Spinelli, S. V.; Soncini, F. C. *Mol. Microbiol.* **2007**, *63*, 1307.
(22) Rodrigue, A.; Effantin, G.; Mandrand-Berthelot, M. A. *J. Bacteriol.* **2005**, *187*, 2912.
(23) Liesegang, H.; Lemke, K.; Siddiqui, R. A.; Schlegel, H. G. *J. Bacteriol.* **1993**, *175*, 767.
(24) Schmidt, T.; Schlegel, H. G. *J. Bacteriol.* **1994**, *176*, 7045.
(25) Nies, D. H. *FEMS Microbiol. Rev.* **2003**, *27*, 313.
(26) Mukhopadhyay, R.; Rosen, B. P.; Phung, L. T.; Silver, S. *FEMS Microbiol. Rev.* **2002**, *26*, 311.

Now it is interesting to explore the fate of bacterial cells after their exposure to metal salts. For this purpose, we imaged the control and Co acetate treated *Brevibacterium casei* cells (fixed using gluteraldehyde as explained in the Supporting Information (Materials and Methods section) after 24, 48, and 72 h. The results are presented in Figures 7 and 8. In the case of control samples, it can be observed that morphology of cells remain unaltered even after 72 h (Figures 7A,B,D and 8F). On the other hand, the bacterial cells which were exposed to the precursor salt solution tend to aggregate or form clusters (Figures 7C and 8E,G), and this tendency increases gradually until 72 h compared to control cells where individual cells are clearly visible even after 72 h. This behavior can be attributed to a kind of stress response where many bacterial strains produce excess extracellular exopolysaccharide, slime, or form capsule to protect themselves against metal ions. Capsule, slime, and bacterial acidic EPS are known to bind and concentrate metal ions and are therefore thought to play a role in the ameliorating metal toxicity.[27,28] These secondary metabolites enforce isolated cells to clump together to form aggregates.[29] It is believed that in these self-organized colonies bacteria can be more resistive to the external stress in comparison to the suspension. Once under the external stress (such as metal ions, food scarcity, antibiotics, adverse environmental conditions, etc.) the bacteria communicate with each other following various mechanisms to cope and survive by exhibiting sophisticated cooperative structural assemblies to behave like a multicellular organism. The organizational behavior which is a protective mechanism shown by microbes while under stress is mediated by the long-range biochemical interactions such as quoram sensing, chemotactic signaling, collective activation/deactivation of genes, and sometimes exchange of genetic material.[30,31]

(27) Zhang, Y.; Jock, S. K.; Geider, *Mol. Genet. Genomics* **2001**, *264*, 732.
(28) Richau, J. A.; Choquenet, D.; Fialho, A. M.; Correia, I. *Res. Microbiol.* **1997**, *148*, 251.
(29) Tang, Y. J.; Ashcroft, J. M.; Chen, D.; Min, G.; Kim, C.-H.; Murkhejee, B.; Larabell, C.; Keasling, J. D.; Chen, F. F. *Nano Lett.* **2007**, *7*, 754.
(30) Jacob, E. B.; Becker, I.; Shapira, Y.; Levine, H. *Trends Microbiol.* **2004**, *12*, 366.
(31) Jacob, E. B.; Cohen, I.; Golding, I.; Gutnick, D. L.; Tcherpakov, M.; Helbing, D.; Ron, I. G. *Physica A* **2000**, *282*, 247.

Native-PAGE profile comparison shows (presented in Figure 9) that most of the proteins are overexpressed in comparison to the control. We believe that the overexpression of these proteins is probably due to the stress response of bacterial cells after exposure to precursor salt. However, some proteins which are not indispensable in this process are not secreted by the treated cells (E). Here it is important to check whether the presence of the *Brevibacterium casei* cells is required for the synthesis process (whether the cells actually participate in the synthesis). We performed a simple test to confirm it. We took the extracellular proteins from the cells after giving them osmotic shock, and we used the same proteins (with out the presence of cells) and reacted with the cobalt acetate solution. However, we did not observe any indication of the synthesis of nanoparticles, which confirms that the presence of the cells is required for the synthesis as mentioned earlier in the text and intracellular biochemistry is playing an important role in the change in the oxidation state as well as formation of single-crystalline Co_3O_4 nanoparticles.

3. Conclusion

To summarize, in this article we demonstrate the immense capabilities of some of the microbes to change the oxidation state of metal ions, in the process of forming stable, protein-functionalized, single- crystalline oxide nanoparticles in pure phase under ambient conditions. This technique holds tremendous potential for the controllable synthesis of other binary and ternary oxide.

Acknowledgment. The authors acknowledge help from Mrs. Suguna Adhyanthaya and Mr. Gholap. The authors also acknowledge Umananda M. Bhatta and P. V. Satyam for their help in HRTEM measurements. U.K. acknowledges help from Council for Scientific and Industrial Research, India, for financial help. P.P. acknowledges the funding from the British Council and from Department of Science Technology (grant under Nano mission).

Supporting Information Available: Materials and Methods and Characterization Techniques sections, FTIR spectra, and phylogenetic tree of marine bacterium used for nanocrystall synthesis. This information is available free of charge via the Internet at http://pubs.acs.org.

CM702727X